

FAST COMPUTATION OF REGION HOMOGENEITY WITH APPLICATION IN A SURVEILLANCE TASK

Uwe Knauer and Beate Meffert

Computer Science Institute, Signal Processing and Pattern Recognition Group
Humboldt-Universität zu Berlin
Unter den Linden 6, 10099 Berlin, Germany
knauer@informatik.hu-berlin.de, meffert@informatik.hu-berlin.de
<http://www.informatik.hu-berlin.de/sv>

Commission V/5

KEY WORDS: segmentation, image classification, homogeneity, image processing

ABSTRACT:

A real-time segmentation of images requires features which are fast to calculate and a segmentation procedure which can fastly classify pixels or regions with respect to these features. Automatic surveillance of a honeybee comb requires the segmentation of homogeneous image regions. Such regions correspond to visible brood cells while the regions which are covered by a crowd of bees appear non-homogeneous. In this paper a novel and efficient way to calculate an existing homogeneity feature is presented. Second, it is extended to a novel feature and empirical results are provided which show improvements over the basic homogeneity value. Third, a simple but effective segmentation procedure is presented and segmentation results are provided.

1 INTRODUCTION

The need for fast and reliable segmentation exists in many computer vision applications. Surveillance applications such as the monitoring of traffic scenes or the monitoring of animals in behavioral studies are typical examples. For us, this need has arisen from implementing a video based monitoring system for the support of biological studies. These studies aim to fight one of the biggest threats for the native honeybee *Apis mellifera*: the mite *Varroa destructor*. The varroa mites are external honeybee parasites. The infestation of a colony is a serious problem because it is not possible to cure an afflicted colony without the use of acaricide agents which lead to unwanted residues in wax and honey. Current research in the field of apiculture focuses on the genetic selection of hygienic bees (Bienefeld and Arnold, 2004) for blocking the mites. However, the selection of hygienic bees requires a time consuming observation of the combs. Processing all the material that is typically recorded for a period of one week (24 hours a day) by a human expert requires at least twice of the recorded period. Therefore, it would be helpful to develop algorithms for an automated observation of the combs and for the detection of the hygienic bees. Fig.1 shows a small region of the observed comb.



Figure 1: Slice of an image from the observed beehive. The real-time assessment of the brood cells in the presence of bees requires fast and robust segmentation.

To show the generality of the approach, we provide segmentation results for two traffic monitoring scenes. The feature seems to be very robust since only the patch size had to be adapted. However, we expect that restricting the analysis to regions of interest, using different patch sizes to account for the cameras viewing angle, or the combination with a background model will further improve segmentation.

The contributions are as follows. First, we present a novel and efficient way to calculate an existing homogeneity feature. Second, we extend it to a novel feature and provide empirical results which show improvements over the default homogeneity value. Third, we propose a simple but effective segmentation procedure and provide segmentation results.

2 RELATED WORK

Real-time segmentation of a homogeneous image background in monitoring a honeybee comb requires the application of computational inexpensive features as well as a fast classification method. Traditional background modelling is not applicable since the basic assumption that the combs surface is visible more often than it is occluded by bees is false. The most sophisticated feature sets which are used in semantic segmentation tasks such as HoG (histogram of gradients), matching of bags of words or visual vocabularies does not fulfil the real-time constraint. Image color information can not be used since we are using near-infrared illumination and monochrome cameras. FFT-based and wavelet-based features might have also been of interest. Since relevant properties of the homogeneous background are only captured by low frequency components we did not pursue this approach. In our opinion, the need for a patch based FFT or wavelet transform contradicts the idea of a fast segmentation.

The calculation of the proposed feature (a homogeneity measure) is based on the image gradients. Therefore, it is closely related to other gradient based techniques. One related method is the structure tensor of an image patch and the analysis of its Eigenvalues. It is commonly used to detect low level image features such as edges and corners. If such a method is not restricted to detect only the most prominent points, it can generate a mask which can be further improved to match the results of our proposed method. Principally, calculating the structure tensor for many large and overlapping image patches is an expensive operation. However, it is possible to use a pyramidal approach to speed up calculation. The compatibility of the proposed feature with summed area tables (integral images) is a major benefit and also a contribution

for different real-time image processing tasks. We will show that a traditional definition of homogeneity can be transformed such that it can be calculated in constant time for any upright rectangular image patch.

Our choice of a simple but adaptive threshold operation for image segmentation is motivated by its wide-spread use in industrial applications. There exists a vast number of threshold approaches, but a recent survey revealed that the choice of a best performing method is highly application specific (Sezgin and Sankur, 2004). Therefore, we decided to use a modification of the well known Otsu method which on average provides a high performance level. Region growing, split-and-merge algorithms, and graph based segmentation are different approaches to image segmentation. Typically, they iterate until convergence of some optimization criterion and therefore can not ensure a fixed processing time.

3 DATASETS

We have selected five datasets from a honeybee monitoring to illustrate our method and to assess its performance.

Dataset 1 consists of 10,200 images of brood cells. It has been first used to assess the performance and parametrization of different classification algorithms which discriminate between three typical states of brood cells (Knauer et al., 2007). Here, it is reused to evaluate the performance of the proposed homogeneity feature in comparison to other feature sets.

The datasets 2, 3, and 4 are short video sequences from three different experiments with different cameras, illumination, and numbers of bees. They are used for evaluation of the segmentation performance.

Dataset 5 is a set of 26 manually segmented images from different experiments. It is used to assess the performance of the proposed segmentation method in comparison to ground truth data as well as to more sophisticated but computational too demanding algorithms.

Datasets 6 and 7 are images from two different traffic monitoring facilities. They are used to illustrate the generality of the approach.

4 FAST HOMOGENEITY-BASED SEGMENTATION

4.1 Theoretical Background

The source of the homogeneity value is the gray value cooccurrence matrix C . The gray value cooccurrence matrix is the two dimensional histogram of the cooccurrence of gray values in an image. It is a classical approach to represent textural features for image classification (Haralick et al., 1973). Given images with 256 (the default 8 bit quantization) or 4096 (12 bit quantization), e.g. in medical or satellite imaging) different values, the cooccurrence matrix has 256^2 or 4096^2 elements. The matrix element $C_{i,j}$ is the (normalized) frequency p of the cooccurrence of gray value i and gray value j in image I :

$$p(I_{x_1,y_1} = i, I_{x_2,y_2} = j | (x_2, y_2) = N^k(x_1, y_1)). \quad (1)$$

In Eq.(1) N^k denotes a fixed geometrical relationship between image pixels such as the right horizontal neighbor. A different cooccurrence matrix exists for any other geometrical relationship. 338

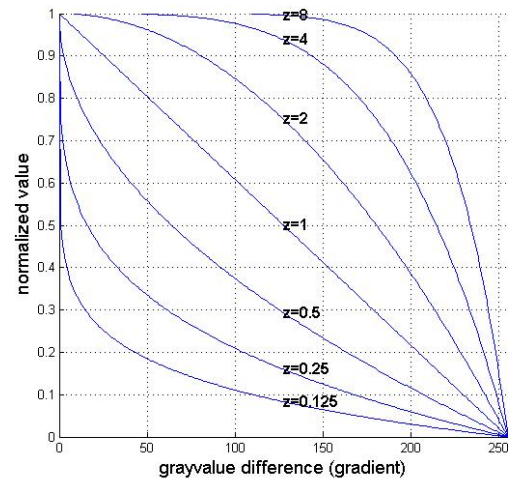


Figure 2: Mappings of gradient values to the interval [0..1] for different choices of the parameter z

Different features that characterize attributes of the texture can be derived from the matrix elements. In (Haralick et al., 1973) the authors presented a list of 14 features. They used the angular second moment as a measure of texture homogeneity.

In Eq.(2) the homogeneity value H is defined differently as proposed by Hochmuth (Hochmuth, 2001). First, all possible gray value differences $|i - j|$ are mapped to the interval [0..1], such that the largest difference value corresponds to zero and the smallest difference corresponds to one. The maximum gray value is denoted by g_{max} . The exponent z controls the importance of certain difference values. Second, the average of all mapped difference values is calculated. The influence of the parameter z on the homogeneity value is visualized in Fig.2.

$$H = \sum_{i=0}^{g_{max}} \sum_{j=0}^{g_{max}} \left[1 - \left(\frac{|i-j|}{g_{max}} \right)^z \right] \cdot C_{i,j} \quad (2)$$

The calculation of the homogeneity measure with Eq.(2) requires the elements of the cooccurrence matrix $C_{i,j}$. According to Eq.(1) $C_{i,j}$ is the frequency of cooccurrence of the gray values i and j . Hence, the cooccurrence matrix is equivalent to the normalized histogram of absolute gradients. Therefore, Eq.(5) and Eq.(6) can be used instead of Eq.(2). Basically, this substitution is familiar to the two ways of calculating the mean value of a gray value image I as illustrated by the following equation:

$$\sum_{g=0}^{255} p(g)g = \frac{1}{wh} \sum_{x=0}^{w-1} \sum_{y=0}^{h-1} I_{x,y}, \quad (3)$$

where $p(\cdot)$ denotes an element of the normalized histogram of image I . We call Eq.(4) a dual representation of Eq.(2) since H no longer depends on the cooccurrence matrix. The variables w and h denote width and height of the image.

$$H_{horz} = \frac{1}{wh} \cdot \sum_{x=1}^w \sum_{y=1}^h \left[1 - \left(\frac{|I_{x,y} - I_{x+1,y}|}{g_{max}} \right)^z \right] \quad (4)$$

The transformation between Eq.(2) and Eq.(4) shows that the homogeneity is basically the weighted average difference image of the original image and a shifted version of the same image. This is important because the mean value of arbitrary rectangular regions can be calculated efficiently.

$$H_{horz} = 1 - \frac{1}{whg_{max}^z} \cdot \sum_{x=1}^{w-1} \sum_{y=1}^h |I_{x,y} - I_{x+1,y}|^z \quad (5)$$

The cooccurrence of gray values should not be investigated in a single direction only. Therefore, Eq.(6) is used to calculate the homogeneity for the vertical relationship.

$$H_{vert} = \frac{1}{wh} \cdot \sum_{x=1}^w \sum_{y=1}^{h-1} \left[1 - \left(\frac{|I_{x,y} - I_{x,y+1}|}{g_{max}} \right)^z \right] \quad (6)$$

Horizontal and vertical homogeneity are combined into a single measure of homogeneity. In Eq.(5) the minimum of both values is used.

$$H = \min(H_{horz}, H_{vert}) \quad (7)$$

The mean of both values is a different option to combine both values.

$$H = \frac{H_{horz} + H_{vert}}{2} \quad (8)$$

In the following section we will discuss how the presented feature H can benefit from Summed Area Tables. The key is the transformation step which has led to Eq.(5) and Eq.(6). Instead of calculating the cooccurrence matrix of each region, the SAT of the shifted difference images allows fast computation of the homogeneity measure for use in texture analysis.

4.2 Fast calculation of homogeneity

Integral images have received lots of attention since they have been introduced by Viola and Jones for fast face detection (Viola and Jones, 2001). They are also known as *Summed Area Tables* (Lienhart and Maydt, n.d.). Lienhart et al. presented an extended feature set as well as an empirical analysis of feature extraction and learning based on integral images (Lienhart et al., 2002, Lienhart and Maydt, n.d.). Wang et al extended the ideas of Viola and Jones to integral histogram images for face detection (Wang et al., 2005). Peihua used integral images for the efficient calculation of color histograms, mean and variance values for color object tracking (Peihua, 2006). Also, Adam and Shimshoni implemented a fast image patch tracker with integral histogram images (Adam et al., 2006). Porikli and coworkers proposed integral images for calculation of region covariance (Tuzel et al., 2006, Porikli, 2006). Recently, Beleznaï et al. used integral images to quickly calculate features for scale-adaptive clustering in a people counting framework (Beleznaï et al., 2007).

The *Summed Area Table* S at the coordinates (x, y) is defined as the sum of all gray values $I_{i,j}$ in the upright rectangular region bounded by the image origin $(0, 0)$ and the coordinates (x, y) .

$$S_{x,y} = \sum_{i=0}^{x-1} \sum_{j=0}^{y-1} I_{i,j} \quad (9)$$

Hence, the recursive definitions are

$$S_{x+1,y} = S_{x,y} + S_{x+1,y-1} - S_{x,y-1} + I_{x,y} \quad (10)$$

$$S_{x,y+1} = S_{x,y} + S_{x-1,y+1} - S_{x-1,y} + I_{x,y} \quad (11)$$

SATs are a well suited data representation for calculating features of rectangular image regions. With Eq.(12) the mean value m for every upright rectangle defined by its upper left corner point A and its lower right corner B can be calculated in constant time with only four lookup operations from the *Summed Area Table*.

$$m = \frac{S_{B_x+1,B_y+1} + S_{A_x,A_y} - S_{A_x,B_y} - S_{B_x+1,A_y}}{(B_x - A_x) \cdot (B_y - A_y)} \quad (12)$$

Remember the dual representation of the homogeneity feature as it was defined by Eq.(4):

$$H_{horz} = \frac{1}{wh} \cdot \sum_{x=1}^w \sum_{y=1}^h \left[1 - \left(\frac{|I_{x,y} - I_{x+1,y}|}{g_{max}} \right)^z \right]. \quad (13)$$

First, we calculate the (per pixel) difference image $|I_{x,y} - I_{x+1,y}|$. Second, we calculate the *SAT* of the resulting difference image. Third, we can query homogeneity values for arbitrary rectangular regions by applying Eq.(12).

4.3 Region homogeneity - Hierarchical application of SATs

Fig. 3 shows how to obtain *region homogeneity*. The upper two blocks correspond to the approach described in the previous section. The combination of the homogeneity values H_{horz} and H_{vert} into a single homogeneity value is depicted as an overall homogeneity $H(I)$. The SAT of this homogeneity map is used to efficiently calculate the average of the homogeneity within any upright rectangular region.

4.4 Segmentation

Fig. 4 shows the proposed segmentation procedure. Homogeneity can be measured at different resolution levels. Here, the patch size has been fixed to 20×20 pixels which approximately corresponds to the size of a brood cell. Remember, that the patch size defines only the coordinates of SAT lookups. Therefore, the patch size can be arbitrarily chosen with respect to the application demands. Moreover it is possible to lookup the patch size for each pixel individually.

The key contribution in this segmentation approach is the use of an adaptive threshold. We decided to use a modified version of the Otsu algorithm. This method finds an optimal threshold that maximizes the between-class variance in a gray value image. The threshold is also required to have a low probability of occurrence. This constraint is an extension of Otsu's method and has been suggested by Ng (Ng, 2006). According to Otsu, the optimal threshold can be determined by maximizing the between-class

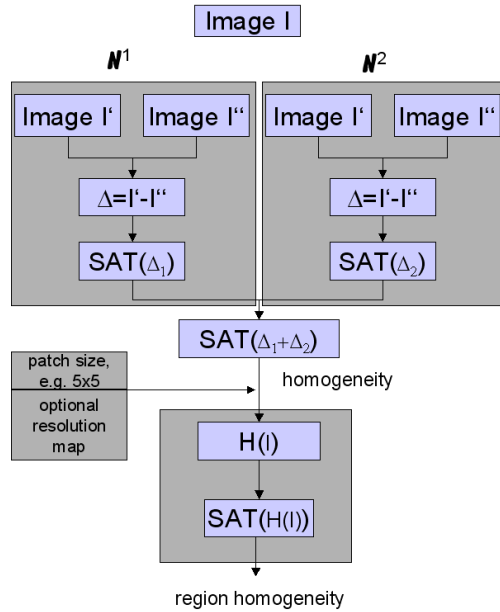


Figure 3: Flow chart of the calculation of *region homogeneity*. N^i denotes different neighborhood relationships. The homogeneity map $H(I)$ is calculated for a fixed patch size, e.g. $H_{5 \times 5}(I)$. Instead an optional patch size map can be used to create $H_{map}(I)$ which combines different resolution levels into a single homogeneity map.

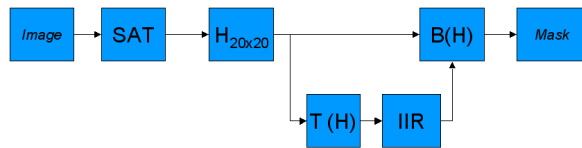


Figure 4: Flow chart of the segmentation procedure. In this example homogeneity (not *region homogeneity*) is calculated at a single resolution level ($H_{20 \times 20}$). The homogeneity map is thresholded. The threshold T is estimated with a modified Otsu algorithm. Recursive filtering (IIR) over time is applied to the threshold value to eliminate segmentation errors. See the text for additional details.

variance. Eq.(14) is an equivalent but simplified formulation from (Ng, 2006).

$$thr = \arg \max_{0 \leq t < B} \{ \omega_1(t) \mu_1^2(t) + \omega_2(t) \mu_2^2(t) \} \quad (14)$$

The gray value distribution which is given by a normalized histogram with B bins is divided into two parts. The probability of occurrence given by the i -th histogram bin is denoted by $p(i)$. The two mean values μ_1 and μ_2 are calculated with Eq.(15) and Eq.(16).

$$\mu_1 = \frac{1}{\omega_1(t)} \sum_{i=0}^t ip(i) \quad (15)$$

$$\mu_2 = \frac{1}{\omega_2(t)} \sum_{i=t+1}^{B-1} ip(i) \quad (16)$$

The two weights ω_1 and ω_2 are defined by Eq.(17) and Eq.(17). 340

$$\omega_1 = \sum_{i=0}^t p(i) \quad (17)$$

$$\omega_2 = \sum_{i=t+1}^{B-1} p(i) \quad (18)$$

The extension to the valley-emphasis method is simple but effective. In Eq.(19) the between class variance is multiplied with a weight $(1 - p(t))$. This term replaces the argument of the arg max function in Eq.(14).

$$(1 - p(t)) \cdot (\omega_1(t) \mu_1^2(t) + \omega_2(t) \mu_2^2(t)) \quad (19)$$

A high probability $p(t)$ results in a low weight. Therefore, the valleys of the gray value distribution are the preferred candidates for threshold selection. The Otsu method can be extended to select multiple thresholds. However, computational time increases exponentially with the number of classes/thresholds. To overcome this limitations Huang and Wang developed a two-stage multithreshold Otsu-method (Huang and Wang, 2009). Among others, this work documents the importance of the contribution of Otsu that he did in the late 1970s.

Reduction of false threshold selection is done by recursive filtering (IIR) of the image based thresholds thr :

$$thr_t = \alpha \cdot thr_{t-1} + (1 - \alpha)thr \quad (20)$$

Typically we set $\alpha = 0.95$. However, segmentation results in Fig. 6 have been obtained without recursive filtering.

5 RESULTS AND DISCUSSION

5.1 Performance of the homogeneity features

In previous work we found that a simple feature space of homogeneity and luminance is easy to interpret, fast to calculate, and provides satisfactory classification performance. However, the rbfSVM on a rich feature set (normalized image) performed much better. We wanted to verify our hypothesis that *region homogeneity* outperforms the traditional homogeneity measure.

Tab. 1 shows the overall performance of different classifiers (10-fold cross-validation) with changing feature sets. The task was to discriminate between visible and occluded brood cells. The parameters of the different classifiers (if exist) have been optimized by systematically testing within practical boundaries. The abbreviation d_{min} denotes the minimum Mahalanobis distance between a feature vector and the mean class vector. It is used as a fast and simple decision rule in the existing monitoring system and provides a lower bound on the overall accuracy of the classifiers. The upper bound is given by the performance of rbfSVM in a 121-dimensional feature space. Boosted decision trees and Random Forest classifiers reach a comparable level of performance as rbfSVM but require a high number of base classifiers.

The results show an error rate reduction of approximately 3 % by using *region homogeneity* instead of homogeneity. The low dimensionality of the feature space also allows to use more sophisticated classification methods without a drastic loss in runtime performance. Using *rbfSVM* instead of a minimum distance classifier an error rate reduction of approximately 10 % can

	H	regionH	18-dim	121-dim
d_{min}	82.22 %	84.93 %	86.56 %	-
rbfSVM	90.8 %	91.09 %	91.59 %	94.3 %
linSVM	82.4 %	85.46 %	88.62 %	84.46 %
polSVM	-	89.92 %	88.89 %	85.04 %

Table 1: Comparison of classification results for different SVM kernel functions and different feature sets (dataset 1). The results of a minimum distance classifier d_{min} are given as a reference.

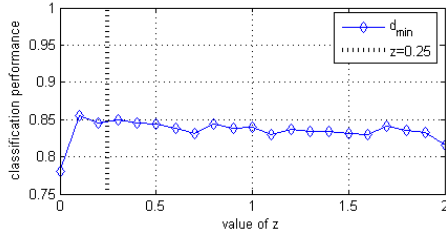


Figure 5: Classification performance as a function of the parameter z (dataset 1)

be achieved. Furthermore, the performance in the 2-dimensional feature space keeps up with the performance in a 18-dimensional rich feature space. The usefulness of *region homogeneity* justifies the need for an efficient computation which has been proposed above. For a list of the 18 features see (Knauer et al., 2007).

Fig. 5 justifies the choice of $z = 0.25$ which has been used throughout the experiments. For the given classification task only a minor dependency on the parameter z exists. However, a smaller value of z gives slightly better results. In this case, Fig. 2 shows a fast and strong negative slope of the homogeneity value for increasing gradient values.

5.2 Performance of the segmentation procedure

It was shown in the previous section that the feature *region homogeneity* reduces the gap in classification performance between the fastest and the best classification method. The task was to classify image patches showing occluded and visible brood cells. This is in accordance with the assumption that the positions and extends of the brood cells are known. An important aspect in our application is the detection of smallest changes on the combs surface. These openings are initiated by only a few hygienic bees which have to be identified. We are also interested in solving the same classification task at the image level instead of the brood cell level. This has several reasons. First, to know where the comb is not occluded is beneficial for other tasks such as bee tracking. Second, changes that occur at brood cell boundaries can be detected more reliable. Third, the segmentation results can be combined to create a up-to-date background image in the presence of a crowd of bees. Fourth, using fast computation of homogeneity in first experiments in other fields (e.g. traffic monitoring) shows promising results.

Some representative results are shown in Fig. 6. Each row consists of three snapshots from recordings which are taken with different cameras, experimental setups and changing environmental conditions. The threshold is calculated as described above.

Given the manually segmented images of dataset 5 we evaluated the segmentation accuracy of different state-of-the-art classifiers. Tab. 2 lists the average percentage of correctly classified pixels from 10-fold cross-validation.

The results show that the proposed segmentation algorithm provides satisfying results given that a single feature was used for

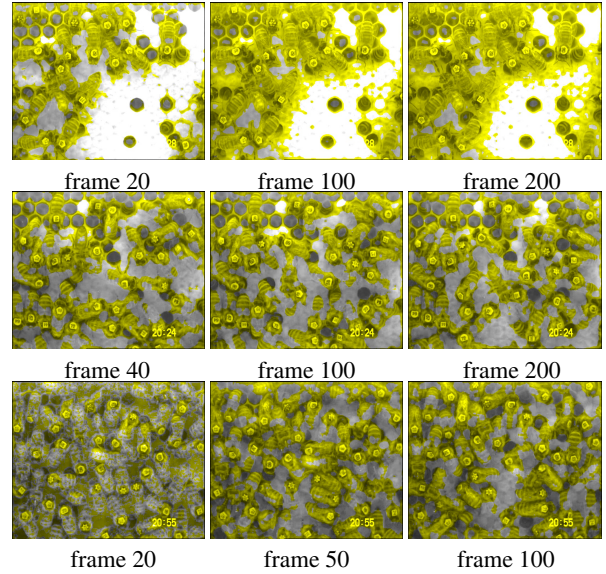


Figure 6: Segmentation results for datasets 2,3, and 5. The yellow colored regions are classified as foreground.

Method	Accuracy (single)	Accuracy (adaboost)
J4.8	79.44 %	86.68 %
k-NN	82.39 %	83.1 %
Otsu (mean)	59.08 %	-
Otsu (standard deviation)	63.78	-
Otsu (proposed)	66.87 %	-

Table 2: Comparison of different classifiers for segmentation of homogeneous image regions (dataset 5) segmentation. The results of an Otsu-based segmentation using different features are also provided in Tab.2.

Because the Spider Toolbox for Matlab was used to assess the segmentation accuracy of different classification algorithms, we do not provide a comparison of segmentation speeds between our C++ implementation of the proposed algorithm and the Matlab functions.

6 CONCLUSIONS AND FUTURE WORK

In this paper we presented the transformation of a homogeneity feature such that the concept of integral images can be applied to speed up its computation. In addition we have shown that an average homogeneity value which we have called *region homogeneity* outperforms the basic homogeneity value in a classification task. Moreover by using integral images this feature can also be calculated efficiently.

We have successfully applied the proposed approach for real-time segmentation in honeybee monitoring. The segmentation algorithm aims to detect those regions which are not crowded by bees. Future work should cover at least two directions. First, it would be beneficial to find efficient algorithms for calculating other region-based features.

Second, the proposed segmentation procedure should be modified and used in other applications. Fig. 7 shows two images from different traffic monitoring facilities. Promising segmentation results are obtained with adaptively thresholding the image into homogeneous and non-homogeneous regions. An important aspect that should be addressed in future work is the use of scale adaptive patch sizes for the calculation of the homogeneity measure. Adapting the patch sizes to the cameras perspective would

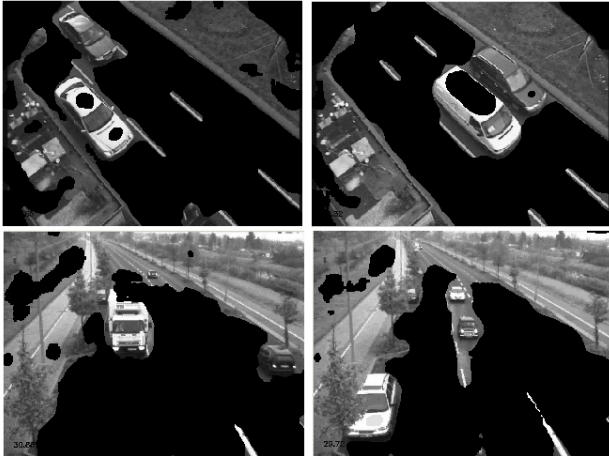


Figure 7: Illustration of the generality of the segmentation approach. Segmentation results in traffic monitoring without a background model and analysis of motion (datasets 6 and 7). $H_{5 \times 5}$ values are used instead of $H_{20 \times 20}$. Segmentation speed approx. 30 fps, image size 320×200 , used hardware: Intel P4, 2.4 GHz.

improve the reliability of the feature. The effects of a missing compensation can be seen clearly from Fig. 7. Homogeneous regions of the streets surface away from the cameras position are falsely classified as non-homogeneous.

ACKNOWLEDGEMENTS

The authors would like to thank the Länderinstitut für Bienenkunde Hohen-Neuendorf and the German Aerospace Center Berlin for providing the datasets.

REFERENCES

- Adam, A., Rivlin, E. and Shimshoni, I., 2006. Robust fragments-based tracking using integral images. In: Proceedings of the 2006 IEEE Computer Society Conference on Computer Vision and Pattern Recognition, Vol. 1, IEEE Computer Society, pp. 798–805.
- Beleznai, C., Sommer, P. and Bischof, H., 2007. Scale-adaptive clustering for object detection and counting. In: Proceedings 10th IEEE International Workshop on Pets.
- Bienefeld, K. and Arnold, G., 2004. Studies on the genetic determination of uncapping of varroa-infested brood cells. In: First European Conference of Apidology, EurBee, pp. 103–104.
- Haralick, R. M., Shanmugam, K. and Dinstein, I., 1973. Textural features for image classification. IEEE Transactions on Systems, Man, and Cybernetics SMC-3(6), pp. 610–621.
- Hochmuth, O., 2001. Collection of formulas for image processing. published online <http://www2.informatik.hu-berlin.de/~hochmuth/download/arbsv34.pdf>.
- Huang, D.-Y. and Wang, C.-H., 2009. Optimal multi-level thresholding using a two-stage otsu optimization approach. Pattern Recognition Letters 30, pp. 275–284.
- Knauer, U., Himmelsbach, M., Winkler, F., Zautke, F., Bienefeld, K. and Meffert, B., 2007. A comparison of classifiers for pre-screening of honeybee brood cells. In: International Conference on Computer Vision Systems.
- Lienhart, R. and Maydt, J., n.d. An extended set of haar-like features for rapid object detection.

Lienhart, R., Kuranov, A. and Pisarevsky, V., 2002. Empirical analysis of detection cascades of boosted classifiers for rapid object detection. Technical report, Microprocessor Research Lab (MRL), Intel Labs.

Ng, H.-F., 2006. Automatic thresholding for defect detection. Pattern Recognition Letters 27, pp. 1644–1649.

Peihua, L., 2006. A clustering-based color model and integral images for fast object tracking. Signal Processing: Image Communication 21, pp. 676–687.

Porikli, F., 2006. Achieving real-time object detection and tracking under extreme conditions. Draft.

Sezgin, M. and Sankur, B., 2004. Survey over image thresholding techniques and quantitative performance evaluation. Journal of Electronic Imaging 13(1), pp. 146–165.

Tuzel, O., Porikli, F. and Meer, P., 2006. Region covariance: A fast descriptor for detection and classification. In: European Conference on Computer Vision.

Viola, P. and Jones, M., 2001. Rapid object detection using a boosted cascade of simple features. In: Proceedings of the IEEE Conference on Computer Vision and Pattern Recognition, pp. 511–518.

Wang, H., Li, P. and Zhang, T., 2005. Proposal of novel histogram features for face detection. In: LNCS 3687 ICAPR, Springer, pp. 334–343.